



D/H Ratio in the Interiors of Rocky Protoplanets Accreting in the Solar Nebula

Hiroaki Saito^{1,2}  and Kiyoshi Kuramoto² 

¹ School of Systems Engineering, Kochi University of Technology, Kami, Kochi, 782-8502, Japan; saito.hiroaki@me.com

² Department of CosmoSciences, Hokkaido University, Sapporo, Hokkaido, 060-0810, Japan

Received 2019 August 30; revised 2019 December 2; accepted 2019 December 3; published 2020 January 23

Abstract

The deuterium/hydrogen (D/H) ratio of primordial water partitioned into a planetary interior seems to be different on Earth and Mars. Water from volcanic rocks originating from Earth's deep mantle has a low D/H ratio with high $^3\text{He}/^4\text{He}$ ratios, implying that it was inherited partially from the solar nebula. In contrast, the D/H ratio of water in the Martian meteorites considered to represent the mantle does not trend toward that of the solar nebula. These differences may be owing to differences in the types of atmospheric structures formed on protoplanets accreting in the solar nebula. Using a 1D radiative-equilibrium model, we analyze the thermal structure of a hybrid-type protoatmosphere in which the solar nebula component dominates the upper layer while a degassed component dominates the lower layer. Our analysis implies Mars-sized protoplanets maintain a hybrid-type protoatmosphere and the D/H ratio of the lower atmosphere resembles that of the building blocks. Conversely, when the mass is larger than Mars-sized, the compositional stratification is collapsed by convective mixing of the solar nebula component with the degassed component, and the D/H ratio approaches that of the solar nebula. This tendency becomes stronger when the planetary mass is larger. If water vapor is distributed through a magma ocean into the planetary interior, Mars-sized protoplanets are likely to reflect the D/H ratios of the building blocks, while larger protoplanets are likely to have acquired a solar-nebula-like D/H ratio.

Unified Astronomy Thesaurus concepts: Mars (1007); Planet formation (1241); Earth (planet) (439); Planetary atmospheres (1244); Planetary science (1255)

1. Introduction

The D/H ratio varies in different water reserves. The D/H ratio of typical carbonaceous chondrite is $\sim 1.6 \times 10^{-4}$ (Robert et al. 2000; Robert 2003) although hydrous minerals in some chondrites locally measured show higher D/H ratios (Deloule & Robert 1995; Deloule et al. 1998; Piani et al. 2015). Cometary water has a wide range of D/H ratios from 1.4×10^{-4} to 6.5×10^{-4} (Bockelée-Morvan et al. 1998; Biver et al. 2016; Alexander et al. 2018), but it generally tends to have a higher D/H ratio than that in typical carbonaceous chondrites. In addition, interstellar water has a high D/H ratio of $\sim 1.7 \times 10^{-3}$ (Cleeves et al. 2014). In contrast, the solar nebula has the lowest D/H ratio of $\sim 2.1 \times 10^{-5}$ (Geiss & Gloecker 1998).

Because the D/H ratio of Earth's oceans (Vienna Standard Mean Ocean Water: $\sim 1.56 \times 10^{-4}$) is almost similar to that of carbonaceous chondrite materials (Alexander et al. 2012; Marty 2012; Sarafian et al. 2014, 2017), one may think that Earth's water originated from carbonaceous chondrites. However, it is rash to draw hasty conclusions, because it has been shown that the D/H ratio can easily increase from three to nine times greater than the primeval value if one considers the hydrogen isotopic-exchange reaction or the hydrodynamic escape of the protoatmosphere (Genda & Ikoma 2008), meaning that in an extreme case, even if only solar nebula water with a very low D/H ratio is supplied, the D/H ratio of water possibly increases up to the value of the present ocean. This implies that the D/H ratio of Earth's proto-ocean was much lower than the present value. Recently, Baffin Island basalt samples, with olivine-hosted glassy melt inclusions, were found to have a lower D/H ratio of about 1.2×10^{-4} ($\delta D = -97\text{‰}$ to -218‰) with higher $^3\text{He}/^4\text{He}$ ratios than Earth's present ocean (Hallis et al. 2015). These samples are

thought to originate from the deep mantle, and Pb–Pb analysis reveals that the formation age of the magma source region is around 4.45–4.55 Gyr ago (Jackson et al. 2010), which corresponds with the formation stage of Earth. This indicates that the source region has not experienced recycling between the surface and interior, either because of plate tectonics and/or the hydrogen isotopic-exchange reaction. Hence, the D/H ratio reported by Hallis et al. (2015) probably reflects the value of primeval water. Because this D/H ratio is within the range of D/H ratios of carbonaceous chondrite ($\delta D = -587\text{‰}$ to $+2150\text{‰}$) (e.g., Kerridge 1985; Alexander et al. 2012), explaining the results of their measurement may be possible even if the only building blocks with such a low D/H ratio accreted on proto-Earth. However, considering the geochemical constraints other than D/H ratio, there are other possibilities; the noble gas (Ne and Xe) anomalies from deep mantle sources of Earth strongly suggest the presence of a solar component (e.g., Trierloff et al. 2000; Holland & Ballentine 2006). Furthermore, some models for the origin of water have suggested the contribution of solar nebula ingassing into Earth's interior (Sharp 2017; Olson & Sharp 2018, 2019; Wu et al. 2018). Therefore, one of the possible causes of the low D/H ratio of the deep mantle is capturing primeval solar nebula water into the planetary interior.

In contrast, the D/H of the Martian interior is still poorly constrained because there are numerous Martian meteorite samples, thought to have originated from the Martian mantle, which display a wide range of D/H ratios; one has a D/H ratio similar to that of typical carbonaceous chondrites ($\delta D \leq 275\text{‰}$) (Hallis et al. 2012; Usui et al. 2012), while in others it is extremely high ($\delta D \leq 4600\text{‰}$; Leshin 2000; Greenwood et al. 2008; McCubbin & Barnes 2019). In the case of Mars, mixing between the surface and the interior is extremely limited owing to the absence of plate tectonics to

date (Watters et al. 2006). Therefore, the measured D/H ratios may correspond to that of primeval water acquired during the formation of Mars, implying that the primary source of Martian water, at least, shows a trend not toward the value of solar nebula but to that of Martian building blocks, which are larger than that of the carbonaceous chondrites.

According to Hf–W analysis of the Martian meteorites, Mars grew rapidly to half its present size within 1.8 ± 1.0 Myr (e.g., Dauphas & Pourmand 2011). This result is in good agreement with theoretical estimates based on the oligarchic growth of planet formation (Kobayashi & Dauphas 2013). According to the latest planetary formation theory, several tens of Mars-sized protoplanets formed in the terrestrial planet region. The protoplanets of Earth’s “embryo” are also thought to have grown more rapidly than Mars. For example, N -body simulations by Raymond et al. (2006) showed that the protoplanets located at 1 au grew up to four times the Mars-sized mass in 2 Myr. The timescale for solar nebula dissipation (<10 Myr) (Kita et al. 2005) suggests that the protoplanets basically accreted within the solar nebula.

When protoplanets become larger than lunar size ($\sim 10^{23}$ kg), volatiles such as H_2O in planetary building blocks begin to degas (hereafter, we refer to this as the “degassed component”), and the degassed component is bounded due to gravity of the protoplanet. Although protoplanets smaller than lunar size possibly degassed if they melted owing to short-lived radionuclides such as ^{26}Al , they retain little of the degassed component because the gravity is too small. Hence, in this study, we ignored its contribution. The protoplanets simultaneously capture the solar nebula component (e.g., Hayashi et al. 1979; Ikoma & Genda 2006). Hence, a hybrid-type protoatmosphere, consisting of the solar nebula in the upper layer and the degassed component in the lower layer, may possibly be formed (Saito & Kuramoto 2018).

A magma ocean may be produced when the surface temperature exceeds the melting point of rock (~ 1500 K) due to the blanketing effect of a thick protoatmosphere (e.g., Matsui & Abe 1986). Because magma absorbs water vapor in proportion to its pressure (e.g., Fricker & Reynolds 1968), the water in the protoatmosphere is expected to be partitioned into the interior of a protoplanet, which thus reflects the D/H ratio of the water vapor. If the degassed component and the solar nebula component are not mixed with each other, the D/H ratio of the protoplanetary interior is likely to correspond to that of the protoplanetary building blocks, i.e., to the degassed component. On the contrary, if they are mixed well, the D/H ratios of the interiors of the protoplanets may show lower D/H ratios, although that depends on the amount of mixing in the protoatmosphere. A low D/H ratio of water is expected to be produced by the hydrogen isotopic-exchange reaction between the low D/H ratio of the hydrogen in the solar nebula and the high D/H ratio of the water in the degassed components: $HD + H_2O \rightarrow HDO + H_2$. The equilibrium constant of this reaction is ~ 1 , and the relaxation timescale to reach this equilibrium is much shorter than the timescale for accretion of the protoplanets (Genda & Ikoma 2008). Therefore, if mixing occurs, the D/H ratio of the water vapor would be the same as that of hydrogen averaged by convective mixing. Another mechanism for producing low D/H water in the protoplanetary building blocks is a redox reaction between the hydrogen in the solar nebula and FeO contained in the magma ocean (Ikoma & Genda 2006; Sasaki 1990). Therefore, we analyze whether the

rise of the conductive mixing or not possibly brings about the difference of the D/H ratio of juvenile water among protoplanets. In this study, we estimate the D/H ratio by analyzing the convective stability of the protoatmospheres forming on different masses of protoplanets.

2. Protoatmosphere Model

2.1. Model Outline

We employ a hybrid-type protoatmosphere model (Saito & Kuramoto 2018) consisting of two layers; an upper layer that is continuously connected to the solar nebula at the Hill radius and which is the domain of the solar nebula component, and a lower layer that is the domain of the degassed component, as shown in Figure 1(a). The solar nebula component is assumed to consist of H_2 and He, and its mean molecular weight is 2.35 (Anders & Grevesse 1989). The D/H ratio of the hydrogen in the solar nebula component is taken to be 2.1×10^{-5} (Geiss & Gloecker 1998). For simplicity, we assumed that no solar nebula dissipation occurs during accretion because the lifetime (~ 10 Myr; Kita et al. 2005) of the solar nebula is likely to be longer than the accretion timescale of protoplanets.

For the building blocks of the protoplanets, we employ the two-component model described by Dreibus & Wanke (1987). Here, we assume that the protoplanets are formed near the orbit of Mars by homogeneous accretion and that their building bricks are 35% CI chondritic material, which is rich in volatile elements and is oxidizing, and 65% enstatite chondritic material, which is depleted in volatile elements and is reducing (Kuramoto 1997). The composition of the degassed component is taken to be $H_2O: H_2: CH_4: CO = 0.15: 0.45: 0.20: 0.20$, which is a typical equilibrium composition, given the CI chondritic H/C ratio and chemical equilibration at an ambient pressure of 100 bar (Kuramoto 1997). The D/H ratio of H_2O and H_2 in the degassed component is taken to be 1.6×10^{-4} , a typical value for CI chondrites (Robert et al. 2000; Robert 2003). According to the two-component model, the mass fraction f_{deg} of the degassed component (CH_4 , CO , H_2 , and H_2O) added per unit mass of the building blocks is estimated to be 4.0 wt%, assuming complete degassing of H and C with the chemical composition described above. However, we used f_{deg} as a free parameter in this study because its value is highly uncertain. For example, the volatiles in the building blocks may be lost before they accrete onto the protoplanets.

2.2. Basic Equations

The complete equations from Saito & Kuramoto (2018) are not repeated here. Instead, we present only those results that are important to the calculations that follow.

The structure of the protoatmosphere satisfies the hydrostatic equilibrium equation,

$$\frac{dp}{dr} = -\frac{GM_p \rho}{r^2}, \quad (1)$$

where p is the pressure, r is the distance from the planetary center, ρ is the averaged density of the protoatmosphere, G is the universal gravitational constant, and M_p is the mass of the protoplanet. Here we neglect the atmospheric self-gravity, because a realistic atmospheric mass is much smaller than the planetary mass. The top of the atmosphere of the protoplanet is

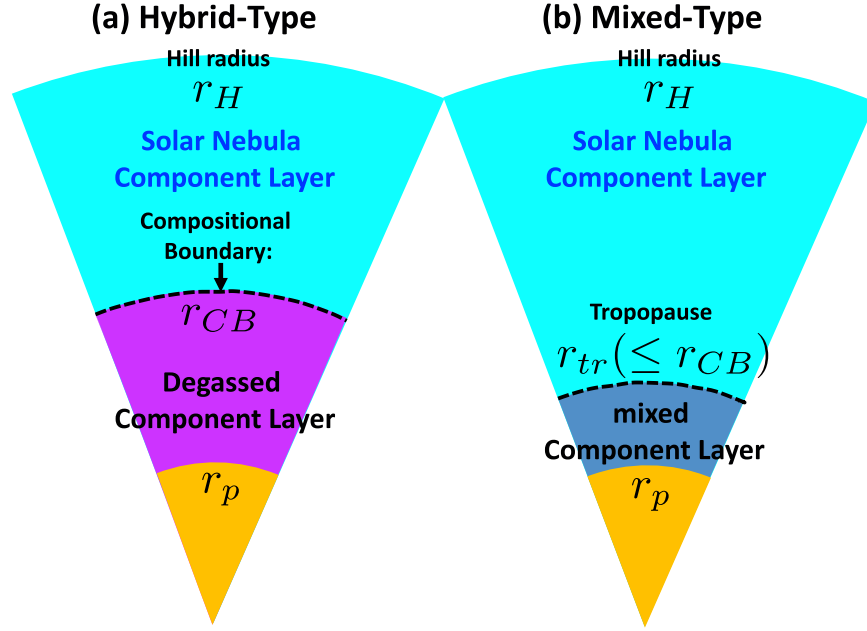


Figure 1. Schematic diagram of (a) a hybrid-type protoatmosphere and (b) a mixed-type protoatmosphere. The uppermost part of the atmosphere is taken to extend to the Hill radius r_H , and the temperature and pressure at the Hill sphere are taken to be $T_H = 178$ K and $p_H = 6 \times 10^{-2}$ (Kusaka et al. 1970). The radius r_{CB} represents the compositional boundary between the solar nebula component layer and the degassed component layer, r_{tr} is the position of the tropopause, and r_p is the radius of the protoplanet. In (a), the upper layer, where $r_{CB} < r < r_H$, consists of the solar nebula component and the lower layer, where $r_p < r < r_{CB}$, consists of the degassed component. The two layers do not mix with each other due to the density gap (Saito & Kuramoto 2018). In (b), the upper layer, where $r_{tr} < r < r_H$, consists of the solar nebula component, while the lower layer, where $r_p < r < r_{tr}$, consists of a mixture of the solar nebula and the degassed components.

taken to be the Hill radius r_H given by

$$r_H = \left(\frac{M_p}{3M_\odot} \right)^{1/3} a, \quad (2)$$

where M_\odot is the mass of the Sun, and a is the heliocentric distance of the protoplanet. The optical depth τ of the atmosphere measured from the Hill radius is expressed as

$$\tau = \int_r^{r_H} \alpha_R dr, \quad (3)$$

where α_R is the Rosseland mean opacity. For the solar nebula component layer, we consider collision-induced absorptions by H_2 and He (Richard et al. 2012) and line absorptions by H_2O calculated from the HITRAN2012 database (Rothman et al. 2013). For the degassed component layer, we add line absorptions by CH_4 and CO from the HITRAN2012 database (Rothman et al. 2013).

2.3. Thermal Structure of the Protoatmosphere

We define the uppermost layer of the protoatmosphere that is in radiative equilibrium to be the stratosphere. At altitudes with $\tau < 2/3$, the temperature distribution of the stratosphere is given by

$$T^4 = T_H^4 + \frac{L}{8\pi r^2 \sigma} \frac{1 + 15\tau/2}{2 + 3\tau/2}, \quad (4)$$

where T is the atmospheric temperature, T_H is the temperature of the background nebula, and σ is the Stefan–Boltzmann constant. The quantity L is the luminosity, which is the net

upward radiative energy flow per unit time,

$$L = \frac{GM_p \dot{M}_p}{r_p}, \quad (5)$$

where r_p is the planetary radius and \dot{M}_p is the accretion rate.

At the altitudes with $\tau \geq 2/3$, the temperature distribution is determined by

$$\frac{dT}{dr} = -\frac{3L}{64\pi\sigma r^2 T^3} \frac{d\tau}{dr}. \quad (6)$$

The lower atmospheric layer, in which the radiative temperature gradient exceeds the adiabatic temperature gradient, is convective. We term the altitude of the radiative–convective boundary to be the tropopause r_{tr} , and the altitude where $r < r_{tr}$ is the troposphere. When water vapor is saturated in the troposphere, the temperature lapse rate obeys the pseudomoist adiabat given by

$$\frac{d \ln T}{d \ln p} = \frac{R + \frac{f_{H_2O} l}{\sum_i f_i T}}{\sum_i f_i c_p^i + f_{H_2O} c_p^{H_2O} + \frac{f_{H_2O} l^2}{\sum_i f_i RT^2}}, \quad (7)$$

where R is the gas constant, l is the molar latent heat for water vaporization, and f_i and c_p^i are the mole fraction and the molar heat capacity at a constant pressure of the non-condensable gas species i ($i = H_2, CO, CH_4$), respectively. When the water vapor is unsaturated, the temperature lapse rate obeys the dry adiabat given by

$$\frac{d \ln T}{d \ln p} = \frac{\gamma - 1}{\gamma}, \quad (8)$$

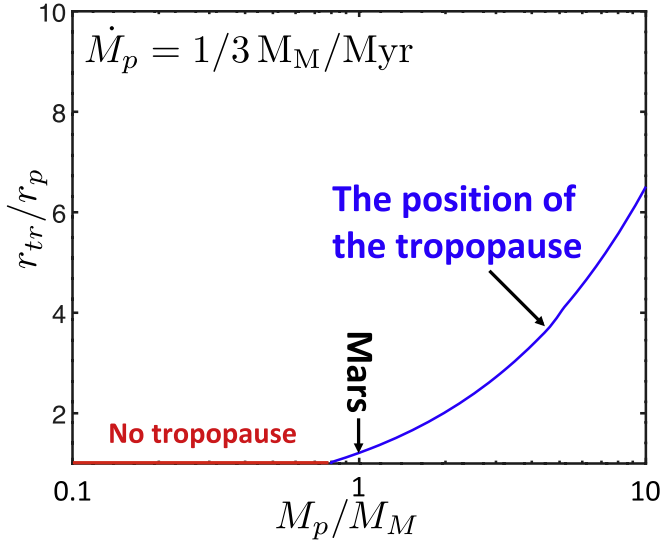


Figure 2. Position of the tropopause as a function of the planetary mass for $\dot{M}_p = 1/3 M_M \text{ Myr}^{-1}$, where M_M is the present mass of Mars. When $M_p/M_M < 0.8$, no tropopause appears in the protoatmosphere because it is optically thin.

where γ is the adiabatic exponent defined by

$$\gamma = \frac{\sum_i f_i c_p^i}{\sum_i f_i c_v^i}, \quad (9)$$

where c_v^i is the molar heat capacity of the gas species i ($i = \text{H}_2\text{O}, \text{H}_2, \text{CO}, \text{CH}_4$) at a constant volume.

3. Convective Mixing Condition

We next consider the condition of convective mixing between the solar nebula component and the degassed component. Here, other mixing processes such as molecular diffusion or the planetesimal collisions are inefficient, at least for Mars-sized protoplanets (Saito & Kuramoto 2018). We thus assume that convection is the main process for mixing the solar nebula component with the degassed component during accretion.

Here, convective mixing is assumed to occur when the tropopause exists in the solar nebula component layer, namely $r_{\text{tr}} \geq r_{\text{CB}}$, under the stratified component assumption. We also assume that the solar nebula component existing between the tropopause and the compositional boundary, and the degassed component existing below the compositional boundary, are readily mixed. For simplicity, we ignore the possibility of the mixing being depressed by the composition gradient. Hereafter, we refer to an atmosphere in which the solar nebula component and the degassed component are mixed as a ‘‘mixed-type’’ protoatmosphere.

First, to analyze the conditions under which a mixed-type protoatmosphere can form, we evaluate the position r_{tr} of the tropopause for a pure solar nebula atmosphere. Figure 2 shows the relationship between r_{tr} and M_p for $\dot{M}_p = 1/3 M_M \text{ Myr}^{-1}$, where M_M is the present mass of Mars. We select this value as a typical accretion rate for a Mars-sized protoplanet (e.g., Dauphas & Pourmand 2011). When $M_p/M_M < 0.8$, no convective mixing occurs because of the high transparency of the atmosphere (e.g., the total atmospheric pressure is 0.42 bar for $M_p/M_M = 0.7$; Saito & Kuramoto 2018), while when $M_p/M_M > 0.8$, convective mixing does occur, because more of

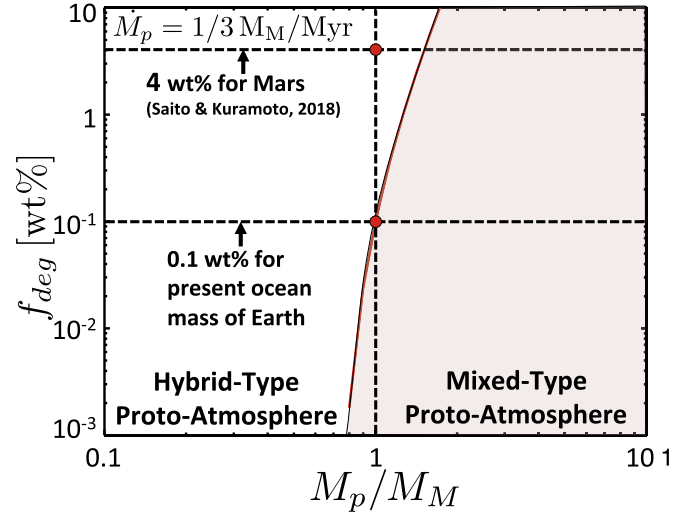


Figure 3. Planetary mass dependence of the threshold value M_{th} converted into the volatile mass fraction f_{deg} . The lower red circle indicates the value of $f_{\text{deg}} = 0.1 \text{ wt\%}$, which is equivalent to the mass M_{oc} of the present ocean of Earth ($\sim 1.4 \times 10^{21} \text{ kg}$). The upper red circle indicates the value of $f_{\text{deg}} = 4 \text{ wt\%}$ that is estimated from the two-component model and used in Saito & Kuramoto (2018).

the solar nebula component is gravitationally bound, and the atmosphere becomes optically opaque.

The structure of the pure solar nebula atmosphere is determined by the energy balance of the radiative flux and the boundary condition given by the temperature and pressure at the Hill radius. If the solar nebula component is replaced by the degassed component where $r < r_{\text{tr}}$, the solar nebula component in the upper layer retains its structure, under the assumption that the components remain stratified; that is, it becomes a hybrid-type protoatmosphere. When $r_{\text{CB}} < r_{\text{tr}}$, convective mixing occurs, and a mixed-type protoatmosphere is formed. In other words, the atmospheric mass of the degassed component at which $r_{\text{CB}} = r_{\text{tr}}$ is the threshold value for classifying a protoatmosphere as hybrid- or mixed-type.

The threshold value M_{th} of the mass of the degassed component is readily obtained as

$$M_{\text{th}} = \int_{r_{\text{tr}}}^{r_p} 4\pi r^2 \rho dr, \quad (10)$$

where we obtain $r_{\text{tr}}^* = r_{\text{CB}}$ from the results shown in Figure 2.

Figure 3 shows the relationship between the volatile mass fraction f_{deg} , which is converted into M_{th} by using the relation $f_{\text{deg}} = M_{\text{th}}/M_p$, and the planetary mass fraction M_p/M_M for $\dot{M}_p = 1/3 M_M \text{ Myr}^{-1}$. When $M_p/M_M = 1$, a hybrid-type protoatmosphere is formed for $f_{\text{deg}} > 0.1 \text{ wt\%}$. However, even at $f_{\text{deg}} = 4 \text{ wt\%}$, based on a two-component model for Mars (Dreibus & Wanke 1987), a mixed-type protoatmosphere is likely to be formed when $M_p/M_M \sim 1.5$. The volatile mass fraction in the building blocks for Earth is expected to be lower than that for Mars, because the orbit of the Earth is closer to the Sun than that of Mars. However, if the current ocean mass of Earth is converted into a volatile mass fraction, its value corresponds to about 0.1 wt%. Hence, the volatile mass fraction is expected to lie in the range $0.1 < f_{\text{deg}} < 4 \text{ wt\%}$, although the uncertainty is high. We therefore expect the D/H ratio of the protoatmosphere to approach that of the solar nebula when a protoplanet grows slightly larger than Mars.

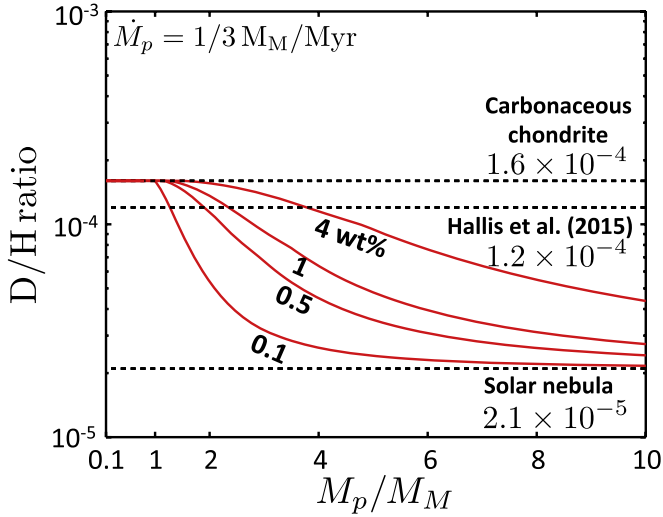


Figure 4. Dependence of the D/H ratio of the lower atmosphere on the planetary mass for $\dot{M}_p = 1/3 M_M \text{ Myr}^{-1}$. The red curves represent the cases $f_{\text{deg}} = 0.1, 0.5, 1,$ and $4 \text{ wt}\%$.

4. Dependence of the D/H Ratio in a Protoatmosphere on Planetary Mass

To evaluate the D/H ratio of the lower atmosphere, we need to compute the amount of the solar nebula component that is mixed with the degassed component layers. We calculate this as follows. First, we calculate r_{tr} as discussed above. The mass M_n of the solar nebula component that exists between r_{tr} and r_{CB} , and the mass M_d of the degassed component, are obtained as follows:

$$M_n = \int_{r_{\text{tr}}}^{r_{\text{CB}}} 4\pi r^3 \rho dr, \quad (11)$$

and

$$M_d = \int_{r_{\text{CB}}}^{r_p} 4\pi r^3 \rho dr. \quad (12)$$

Hereafter, the subscripts n and d denote the solar nebula component and the degassed component layer, respectively. The number densities of hydrogen molecules contained in M_n and M_d are given by

$$n_n = \frac{M_n}{\mu_n} f_{\text{H}_2, n} \quad (13)$$

and

$$n_d = \frac{M_d}{\mu_d} f_{\text{H}_2, d}, \quad (14)$$

respectively, where $f_{\text{H}_2, i}$ ($i = n, d$) are the mole fractions of hydrogen molecules. Assuming that the hydrogen molecules in the solar nebula component layer between the tropopause and the compositional boundary mix completely with the hydrogen molecules contained in the degassed component layer, we can evaluate the average D/H ratio of the mixed-type protoatmosphere $(\text{D}/\text{H})_{\text{mix}}$ as

$$(\text{D}/\text{H})_{\text{mix}} = \frac{\left(\frac{n_n}{n_d}\right)(\text{D}/\text{H})_n + (\text{D}/\text{H})_d}{\left(\frac{n_n}{n_d}\right)(1 - (\text{D}/\text{H})_n) + (1 - (\text{D}/\text{H})_d)}, \quad (15)$$

where $(\text{D}/\text{H})_i$ ($i = n, d$) is the D/H ratio of each layer.

Figure 4 shows the dependence of $(\text{D}/\text{H})_{\text{mix}}$ on M_p/M_M for the fixed accretion rate of $1/3 M_M \text{ Myr}^{-1}$. When the planetary mass is less than a Mars-sized mass, the D/H ratio of the lower atmosphere is similar to that of typical carbonaceous chondrites, regardless of the value of f_{deg} . However, the larger the planetary mass, the more the solar nebula component becomes mixed with the degassed component; the D/H ratio of the lower atmosphere is thus close to that of the solar nebula. For $f_{\text{deg}} = 4 \text{ wt}\%$, the value of the D/H ratio is approximately 4×10^{-5} for an Earth-sized mass. Even if $M_p/M_M = 4$, the D/H ratio is less than that given in Hallis et al. (2015). For $f_{\text{deg}} = 0.1 \text{ wt}\%$, however, the D/H ratio is almost equal to that of the solar nebula when the planetary mass is several times the mass of Mars.

Figure 5 shows the relation between $(\text{D}/\text{H})_{\text{mix}}$ and M_p/M_M for the accretion rates between 0.01 and $1 M_M \text{ Myr}^{-1}$. When the planetary mass reaches $1.5 M_M$, for any value of f_{deg} , the value of the D/H ratio is less than 1.6×10^{-4} ; that is, a mixed-type protoatmosphere is formed. The D/H ratio decreases with increasing planetary mass, while the D/H ratio decreases slowly with an increasing accretion rate. Consequently, the position of the compositional boundary shifts upward due to thermal expansion of the atmosphere at higher accretion rates. As a result, a large amount of hydrogen from the solar nebula component layer is incorporated into the degassed component layer by convective mixing, and the D/H ratio decreases.

For the values of f_{deg} used in this study, we found that the D/H ratio of the protoatmosphere formed on a Mars-sized protoplanet after oligarchic growth is almost the same as that of the carbonaceous chondrites, as shown in Figure 5. This result seems to be compatible with the petrological evidence from Martian meteorites (e.g., Hallis et al. 2012; Usui et al. 2012). On the contrary, according to theoretical studies of planetary formation, Earth was formed by the protoplanets impacting each other several times. When $M_p/M_M = 4$ (Raymond et al. 2006), for instance, the D/H ratio decreases dramatically. When $0.1 < f_{\text{deg}} < 1 \text{ wt}\%$, $(\text{D}/\text{H})_{\text{mix}}$ is much less than the D/H ratio of the Baffin Island basalt samples discussed by Hallis et al. (2015) in the range of $0.01 < \dot{M}_p < 1 M_M \text{ Myr}^{-1}$. When $1 < f_{\text{deg}} < 4 \text{ wt}\%$, $(\text{D}/\text{H})_{\text{mix}}$ decreases moderately compared with cases with lower f_{deg} , because of the large amount of degassed component contained in the lower layer.

In this study, the pressure and temperature of the solar nebula near the orbit of Mars are fixed. If we consider the case for Earth, the pressure and temperature of the solar nebula are expected to be higher, which increases the opacity and promotes convection in the solar nebula component layer. In addition, this tendency becomes stronger when the planetary mass is larger. Hence, convective mixing is expected to occur more easily. To confirm the effect of the pressure and temperature of the solar nebula in more detail, further studies are necessary.

5. D/H Ratio of the Interior of the Protoplanet

We assume that the D/H ratio of the interior of a planet reflects that of the protoatmosphere formed during accretion. In the range of volatile mass fractions we assumed, $0.1 < f_{\text{deg}} < 4 \text{ wt}\%$, a hybrid-type protoatmosphere can be maintained on Mars-sized protoplanets. When $f_{\text{deg}} > 0.1 \text{ wt}\%$, the surface temperature exceeds the melting temperature of rock ($\sim 1500 \text{ K}$) (Saito & Kuramoto 2018) owing to the

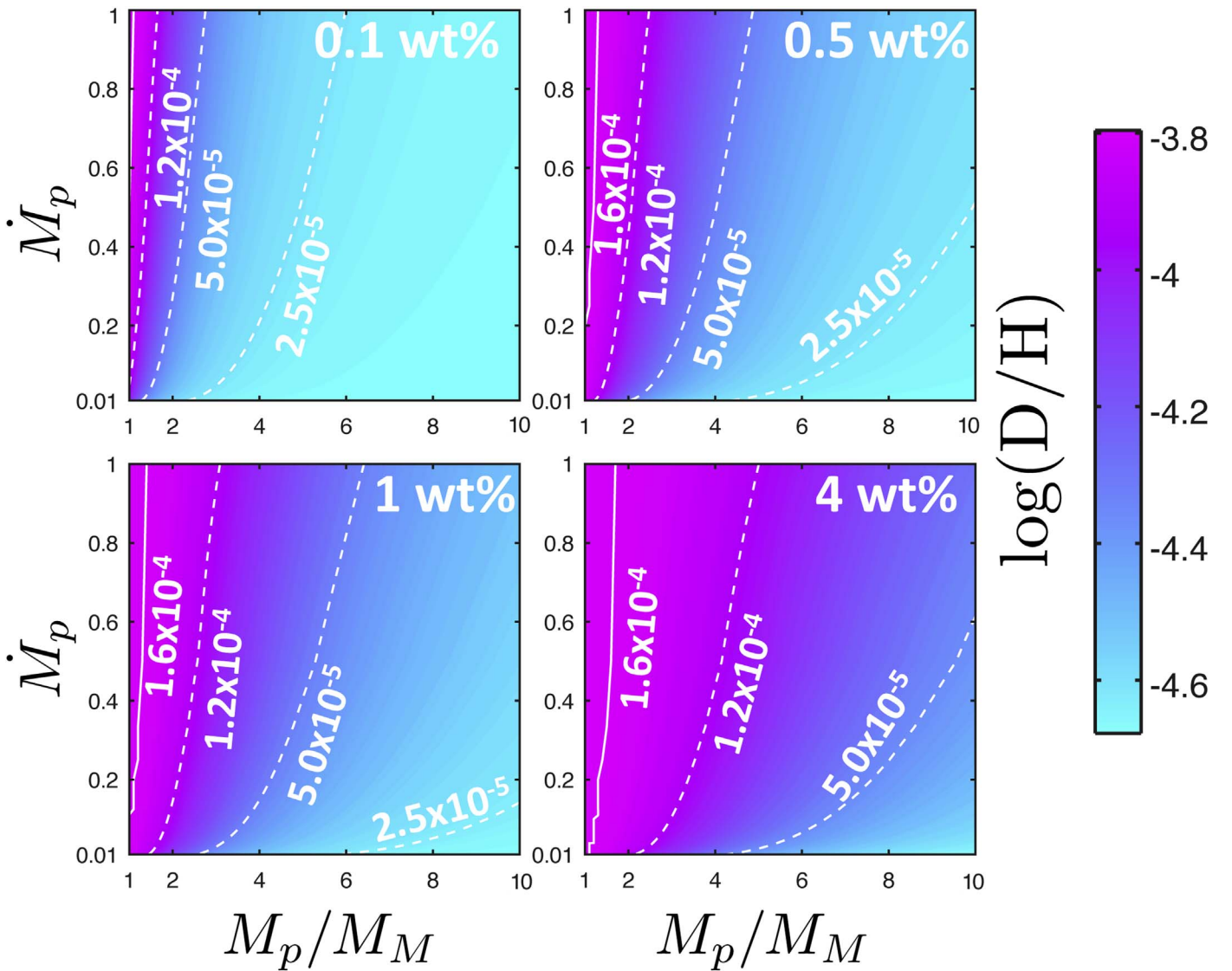


Figure 5. Relationship of the D/H ratio of the lower atmospheric layer to the accretion rate ($0.01 < \dot{M}_p < 1 M_M \text{ Myr}^{-1}$) and the planetary mass ($0.1 < M_p/M_M < 10$). The area to the left of the white solid curve represents the D/H ratio of typical carbonaceous chondrite of 1.6×10^{-4} . The dashed curves and color contours indicate the D/H ratio of the lower atmospheric layer.

blanketing effect. Therefore, in the case of Mars-sized protoplanets, mixing between the degassed and the solar nebula component may be suppressed during accretion, and compositional stratification is then maintained. As a result, part of the water and hydrogen in the degassed component layer is distributed to be absorbed into the interior of a Mars-sized protoplanet, which then acquires the D/H ratio of the carbonaceous chondrites.

On the other hand, because there is great uncertainty in the volatile mass fraction of the planetesimals, the volatile mass fraction may be lower than the range we have assumed. For example, even if a planetary mass is Mars-sized, if $f_{\text{deg}} < 0.1 \text{ wt\%}$, the convective mixing occurs, and the D/H ratio of the lower atmospheric layer takes a nebular-gas-like value. However, in such a case, the blanketing effect is not strong enough to form a magma ocean. In this case, the water absorbed from the protoatmosphere into the interior is extremely limited, because the ground surface is not molten globally. Hence, the water inside a Mars-sized protoplanet is likely to originate mainly from the planetesimals, so the D/H

ratio of the planetary interior resembles that of the typical carbonaceous chondrites.

Although the typical masses of protoplanets before the earlier collisions between protoplanets are generally estimated to lie between the masses of the Moon and Mars, larger masses may be obtained as shown by Raymond et al. (2006), depending on the areal density of the planetesimals. For example, let us consider the case where a protoplanet with a mass of $4M_M$ exists near the orbit of Earth (Raymond et al. 2006). For $f_{\text{deg}} = 0.1 \text{ wt\%}$, equivalent to the mass M_{oc} of the present ocean ($\sim 1.4 \times 10^{21} \text{ kg}$), the D/H ratio is between 3.2×10^{-5} and 2.2×10^{-5} in the range of $0.01 < \dot{M}_p < 1 M_M \text{ Myr}^{-1}$. Even in the case with $f_{\text{deg}} = 4 \text{ wt\%}$ ($\sim 40M_{\text{oc}}$), from the two-component model, we expect the D/H ratio to decrease down to 1.2×10^{-4} as shown in Figure 5. In this case, the ground surface temperature exceeds the melting point of rock, and the protoatmosphere components can be efficiently mixed into the interior of the planet. Thus, when a protoplanet is larger than the size of Mars, the solar nebula component may

have been taken into the planetary interior before the earlier collisions between protoplanets.

6. Conclusion

We have discussed the convective stability of the compositional stratification of hybrid-type protoatmospheres by comparing the position of the compositional boundary with that of the tropopause. If the planetary mass is on the order of the size of Mars, a hybrid-type protoatmosphere is maintained for $f_{\text{deg}} > 0.1$ wt%. We expect the interiors of the protoplanets to acquire water and hydrogen mainly from planetesimals with a D/H ratio similar to those of the carbonaceous chondrites. On the other hand, for a protoplanet four times larger than a Mars-sized mass, the amount of the solar nebula component that is gravitationally bound increases drastically, which causes convective mixing with the degassed component. As a result, a mixed-type protoatmosphere is formed. In this case, the D/H ratio of the mixed component layer approaches that of the solar nebula. Before reaching four times the mass of Mars, the D/H ratio of the planetary interior decreased down to the order of the reported value of 1.2×10^{-4} (Hallis et al. 2015) even if $f_{\text{deg}} = 4.0$ wt%. The interior of protoplanets larger than Mars might thus have acquired water with a low D/H ratio due to convective mixing. These results are one possibility to account for the petrological evidence of differences in D/H ratios of the interior of Mars and Earth.

The authors are grateful to the anonymous reviewer. Additionally, the authors would like to thank Enago (www.enago.jp) for the English language review. This work was supported by MEXT/JSPS KAKENHI grant Nos. 17H06457 and 18K03719.

ORCID iDs

Hiroaki Saito  <https://orcid.org/0000-0001-7937-2971>

Kiyoshi Kuramoto  <https://orcid.org/0000-0002-6757-8064>

References

Alexander, C. M. O'D., Bowden, R., Fogel, M. L., et al. 2012, *Sci*, **337**, 721
 Alexander, C. M. O'D., McKeegan, K. D., & Altwegg, K. 2018, *SSRv*, **214**, 36
 Anders, E., & Grevesse, N. 1989, *GeCoA*, **53**, 197
 Biver, N., Moreno, R., Bockelée-Morvan, D., et al. 2016, *A&A*, **589**, 78

Bockelée-Morvan, D., Gautier, D., Lis, D. C., et al. 1998, *Icar*, **133**, 1
 Cleeves, L. I., Bergin, E. A., Alexander, C. M. O'D., et al. 2014, *Sci*, **345**, 1590
 Dauphas, N., & Pourmand, A. 2011, *Natur*, **473**, 489
 Deloule, E., & Robert, F. 1995, *GeCoA*, **59**, 4695
 Deloule, E., Robert, F., & Doukhan, J. C. 1998, *GeCoA*, **62**, 3367
 Dreibus, G., & Wanke, H. 1987, *Icar*, **71**, 225
 Fricker, E., & Reynolds, T. 1968, *Icar*, **9**, 221
 Geiss, J., & Gloecker, G. 1998, *SSRv*, **84**, 239
 Genda, H., & Ikoma, M. 2008, *Icar*, **194**, 42
 Greenwood, J. P., Itoh, S., Sakamoto, N., Vicenzi, E. P., & Yurimoto, H. 2008, *GeoRL*, **35**, L05203
 Hallis, L. J., Taylor, G. J., Nagashima, K., & Huss, G. R. 2012, *E&PSL*, **359**, 84
 Hallis, L. J., Huss, G. R., Nagashima, K., et al. 2015, *Sci*, **350**, 795
 Hayashi, C., Nakazawa, K., & Mizuno, H. 1979, *E&PSL*, **43**, 22
 Holland, G., & Ballentine, C. J. 2006, *Natur*, **441**, 186
 Ikoma, M., & Genda, H. 2006, *ApJ*, **648**, 696
 Jackson, M., Carlson, R. W., Kurz, M. D., et al. 2010, *Natur*, **466**, 853
 Kerridge, J. F. 1985, *GeCoA*, **49**, 1707
 Kita, N. T., Huss, G. R., Tachibana, S., et al. 2005, in ASP Conf. Ser. 341, Chondrites and the Protoplanetary Disk, ed. A. N. Krot, E. R. D. Scott, & B. Reipurth (San Francisco, CA: ASP), 558
 Kobayashi, H., & Dauphas, N. 2013, *Icar*, **225**, 122
 Kuramoto, K. 1997, *PEPI*, **100**, 3
 Kusaka, T., Nakano, T., & Hayashi, C. 1970, *PTHPh*, **44**, 1580
 Leshin, L. A. 2000, *GeoRL*, **27**, 2017
 Marty, B. 2012, *E&PSL*, **313**, 56
 Matsui, T., & Abe, Y. 1986, *Natur*, **319**, 303
 McCubbin, F. M., & Barnes, J. J. 2019, *E&PSL*, **526**, 115771
 Olson, P., & Sharp, Z. D. 2018, *E&PSL*, **498**, 418
 Olson, P., & Sharp, Z. D. 2019, *PEPI*, **294**, 106294
 Piani, L., Robert, F., & Remusat, L. 2015, *E&PSL*, **415**, 154
 Raymond, S., Quinn, T., & Lunine, J. I. 2006, *Icar*, **183**, 265
 Richard, C., Gordon, I. E., Rothman, L. S., et al. 2012, *JQSRT*, **113**, 1276
 Robert, F. 2003, *SSRv*, **106**, 87
 Robert, F., Gautier, D., & Dubrulle, B. 2000, *SSRv*, **92**, 201
 Rothman, L., Gordon, I. E., Babikov, Y., et al. 2013, *JQSRT*, **130**, 4
 Saito, H., & Kuramoto, K. 2018, *MNRAS*, **475**, 1274
 Sarafian, A. R., Nielsen, S. G., Marschall, H. R., McCubbin, F. M., & Monteleone, B. D. 2014, *Sci*, **346**, 623
 Sarafian, A. R., Hauri, E. H., McCubbin, F. M., et al. 2017, *RSPTA*, **375**, 20160209
 Sasaki, S. 1990, *Origin of the Earth* (Oxford: Oxford Univ. Press)
 Sharp, Z. D. 2017, *ChGeo*, **448**, 137
 Tieloff, M., Kunz, J., Clague, D. A., Harrison, D., & Allègre, C. J. 2000, *Sci*, **288**, 1036
 Usui, T., Alexander, C. M. O'D., Wang, J., Simon, J. I., & Jones, J. H. 2012, *E&PSL*, **357**, 119
 Watters, T. R., Leuschen, C. J., Plaut, J. J., et al. 2006, *Natur*, **444**, 905
 Wu, J., Desch, S. J., Schaefer, L., et al. 2018, *JGRE*, **123**, 2691